Journal of Magnetism and Magnetic Materials 126 (1993) 71–75
North-Holland

journal of magnetism and magnetic materials

X-ray diffraction analysis of lattice strain in metallic superlattice films

N. Nakayama [a], L. Wu [b], H. Dohnomae [b], T. Shinjo [b], J. Kim [c] and C.M. Falco [c]

[a] *Department of Chemistry, Faculty of Science, Kyoto University, Kyoto 606-01, Japan*
[b] *Institute for Chemical Research, Kyoto University, Uji 611, Japan*
[c] *Optical Sciences Center and Department of Physics, University of Arizona, Tucson, AZ 85721, USA*

In-plane lattice spacings of [Au(xÅ)/Ni(xÅ)] and [Pd(xÅ)/Cu(xÅ)] superlattice films with $[111]_{fcc}$ textures and large lattice misfits have been measured by X-ray diffraction. With decrease of superlattice period ($\Lambda = 2x$), Au and Pd layers are compressed whereas Ni and Cu layers are expanded. The observed lattice spacings (d_{220}) of the individual layers vary almost linearly depending on $1/\Lambda$. The lattice spacings of two constituent layers become equal in a Au/Ni superlattice with $\Lambda = 8$ Å ($d_{220} = 1.371$ Å) and a Pd/Cu superlattice with $\Lambda = 14$ Å ($d_{220} = 1.337$ Å).

1. Introduction

Quantitative evaluations of lattice strain from X-ray diffraction measurements are necessary to clarify the origin of perpendicular magnetic anisotropy or supermodulus effect observed for metallic superlattice films. Many studies on the lattice strain along the growth direction have been reported. For example, the correlations between the average lattice spacing and the elastic anomaly are of great interest [1]. However, no systematic X-ray diffraction study on the thickness dependence of the in-plane lattice strain has been reported. Direct X-ray diffraction measurements of in-plane lattice spacings are not so easy because most of the substrates are not transparent for X-ray. Measurements in the transmitting geometries are possible only for samples of which substrates were removed after deposition [2] or those deposited on very thin substrates [3]. However, if the films are single-crystalline, the measurements of off-axial satellite reflections in the asymmetrically reflecting geometries give accurate in-plane lattice spacings [2,4,5]. The measurements in the grazing incidence geometries are also possible even for textured superlattices [6,7].

Supermodulus effects of Au/Ni and Pd/Cu superlattice films have long been investigated [8–10]. All the constituent metals in these superlattices have fcc structures. For Au/Ni and Pd/Cu superlattice films with [111] textures, the in-plane lattice misfits are 14% and 9%, respectively. Because of the large lattice misfits, the thickness dependences of in-plane lattice spacings and their correlation with the average lattice spacing in the growth direction are of great interest. In this paper, the results from the X-ray diffraction measurements of in-plane lattice spacings are presented for both Au/Ni and Pd/Cu superlattices.

Correspondence to: Dr. N. Nakayama, Present address: Faculty of Engineering, Yamaguchi University, Ube 755, Japan. Tel. (+81) 836-31-5100, Fax. (+81) 836-35-9403.

2. Experimental

Au/Ni superlattice films were prepared by an ultra-high vacuum deposition method using electron beam heating systems [11]. Pd/Cu superlattice films were prepared by a magnetically enhanced dc-triode sputtering method [10]. Substrates for Au/Ni superlattices were SiO_2 glass plates and polyimide films. Substrates for Pd/Cu superlattices were Al_2O_3 00.1 single crystals. The designed thicknesses of superlattice films were $[Au(x\text{Å})/Ni(x\text{Å})]_n/Au(250\text{Å})$ and $[Pd(x\text{Å})/Cu(x\text{Å})]_n/Pd(x\text{Å})$. Superlattice periods ($\Lambda = 2x$) ranged from 8 to 106 Å. The total thicknesses were in the range from 1250 to 2000 Å for Au/Ni and nearly equal to 4000 Å for Pd/Cu, respectively. The compositions were measured by Rutherford backscattering spectrometry.

X-ray diffraction measurements were performed using Cu-Kα radiation from a rotating anode type generator and a four-circle diffractometer. The diffractometer was equipped with an incident beam monochromator and a diffracted beam analyzer of graphite 00.2 single crystals. The beam size was 0.5×4 mm^2. The θ–2θ scan profiles with the scattering vector (Q) perpendicular to the film plane were measured for all the samples to investigate the structures in the growth direction. In-plane lattice spacings were measured in a symmetrically transmitting geometry (fig. 1(a)) for Au/Ni superlattices deposited on 7.5 μm thick polyimide films. For the in-plane measurements of Pd/Cu superlattices deposited on thick Al_2O_3 substrates, a

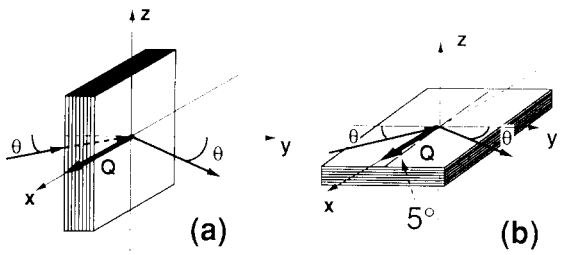

Fig. 1. Diffraction geometries for the X-ray diffraction measurement of in-plane lattice spacings. (a) Symmetrically transmitting geometry for Au/Ni superlattices. (b) Grazing incidence geometry for Pd/Cu superlattices.

grazing incidence method was used. The films were tilted from the diffracting plane with an angle of 5° (Fig. 1(b)).

The accuracy of peak positions in these two in-plane geometries were checked by the measurements for a 250 Å thick and [111] textured Au film.

3. Results and discussion

Figs. 2(a) and (b) show X-ray diffraction profiles with the scattering vectors perpendicular to the film plane for two typical samples. Their designed structures are [Au(4 Å)/Ni(4 Å)]$_{210}$/Au(250 Å) and [Pd(7 Å)/Cu(7 Å)]$_{229}$, respectively. Sharp satellite reflections are observed around the $(111)_0$ and $(222)_0$ fundamental reflections indicating $[111]_{fcc}$ textures. X-ray

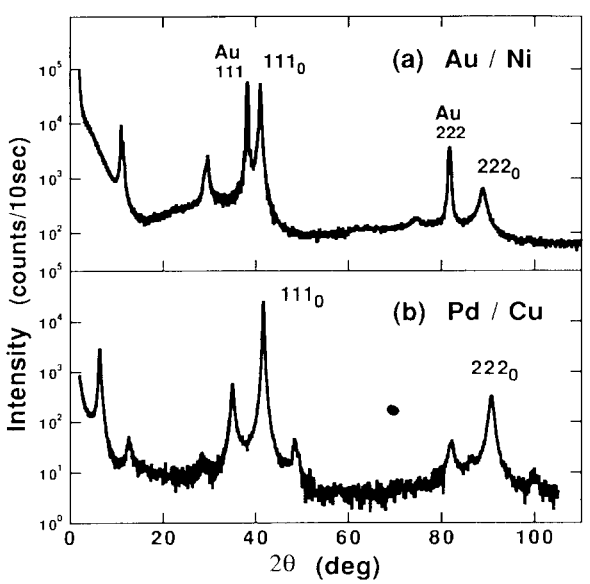

Fig. 2. X-ray diffraction profiles with the scattering vector perpendicular to the film plane for (a) [Au(4 Å)/Ni(4 Å)]$_{210}$/Au(250 Å) and (b) [Pd(7 Å)/Cu(7 Å)]$_{229}$ superlattices.

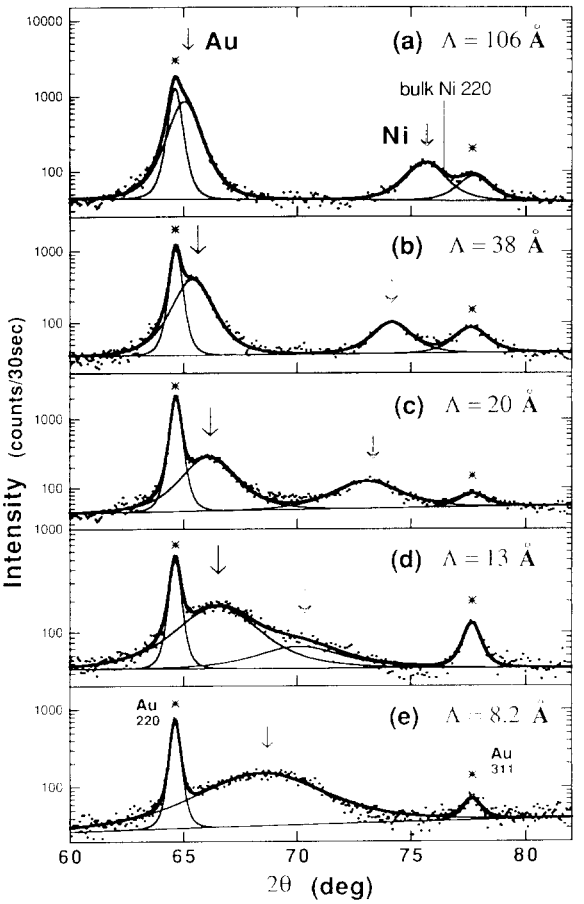

Fig. 3. X-ray diffraction profiles with the scattering vector in the film plane for [Au(xÅ)/Ni(xÅ)]$_n$/Au(250 Å) superlattices observed in the transmitting geometry. Line plots are the results of profile fitting to estimate peak positions and widths. A modified Lorentzian profile function $[1+a(x-x_0)^2]^{-2}$ was assumed.

diffraction patterns of other samples also indicated their $[111]_{fcc}$ textures. However, observed textures were fiber type ones. A cross-sectional TEM study of the present Au/Ni superlattices has revealed that films are composed of small crystallites with random orientations in the film plane (ref. [11]). The [111] directions of crystallites are also distributed. For [Au(4 Å)/Ni(4 Å)]$_{201}$/Au(250 Å) and [Pd(7 Å)/Cu(7 Å)]$_{229}$ superlattices, the rocking curves of $(111)_0$ fundamental reflections showed their full widths at half maximum (FWHM) equal to 6° and 9°, respectively.

Fig. 3 shows X-ray diffraction profiles with the scattering vectors in the film plane for [Au(xÅ)/Ni(xÅ)]$_n$/Au(250 Å) superlattices. The sharp peaks marked by asterisks are those from the 250 Å-thick Au buffer layers. For $[111]_{fcc}$ textures, 220 reflection is the

observable one at the smallest 2θ position. No peak was observed in the 2θ range less than 60°. Because of the wide distribution in the [111] direction of crystallites, Au 311 peaks were observed. If there exits no distribution of the [111] direction, 311 reflection is located at an angle of 80° measured from the [111] fiber axis (ref. [11]).

Diffraction patterns for samples with $\Lambda \geq 13$ Å show two peaks from Au and Ni layers in the superlattices. Peak positions are different from those of bulk metals even when $\Lambda = 106$ Å. Peaks from superlattice are much broader than those from the buffer layers. The observed peak widths for a sample with $\Lambda = 106$ Å give coherence lengths of about 60 Å calculated from the Scherrer formula. With decrease of superlattice period, two peaks from superlattices shift to decrease the peak separation. The Ni layers are expanded and the Au layers are compressed. The peak width increases markedly with decreasing Λ. A sample with $\Lambda = 8.2$ Å shows a very broad peak from superlattice, of which FWHM gives a coherence length of 20 Å. Although the observed in-plane lattice spacings of Au and Ni layers are nearly equal (1.371 Å), the short coherence length suggests that in plane structure is still incoherent even when $\Lambda = 8.2$ Å.

Fig. 4 shows diffraction profiles for $[Pd(x\text{Å})/Cu(x\text{Å})]_n$ superlattices observed in the grazing incidence geometry. For samples with $\Lambda \geq 19$ Å, the diffraction patterns show two peaks from Pd and Cu layers. Small lattice strains are indicated even for a sample with $\Lambda = 102$ Å. With decrease of Λ, peaks shift to decrease the peak separation similarly to the Au/Ni superlattices. The Pd layers are compressed and the Cu layers are expanded. For a sample with $\Lambda = 14$ Å, the diffraction pattern shows a single peak, of which FWHM gives a coherence length of 60 Å. In-plane lattice spacings of Pd and Cu layers are equal to be 1.337 Å. In contrast to the Au/Ni superlattice with $\Lambda = 8$ Å, the Pd/Cu superlattice with $\Lambda = 14$ Å has a fairly coherent in-plane structure.

Observed in-plane (220) lattice spacings and peak widths for both Au/Ni and Pd/Cu superlattices were plotted as a function of $1/\Lambda$ in fig. 5(a) and (b). The lattice spacings in the bulk metals are plotted at $1/\Lambda = 0$. The observed in-plane (220) lattice spacings are almost linearly dependent on $1/\Lambda$ when two distinct peaks are observed. The dotted lines in fig. 5(a) are the least squares fits for the data of samples showing distinct two peaks. Similar linear $1/\Lambda$ dependences of in-plane lattice strains have been reported also for Ni/Mo superlattices [7].

For Au/Ni superlattices, the least squares fitted lines of Au(220) and Ni(220) lattice spacings cross at around $\Lambda = 8$ Å where the observed profile shows a

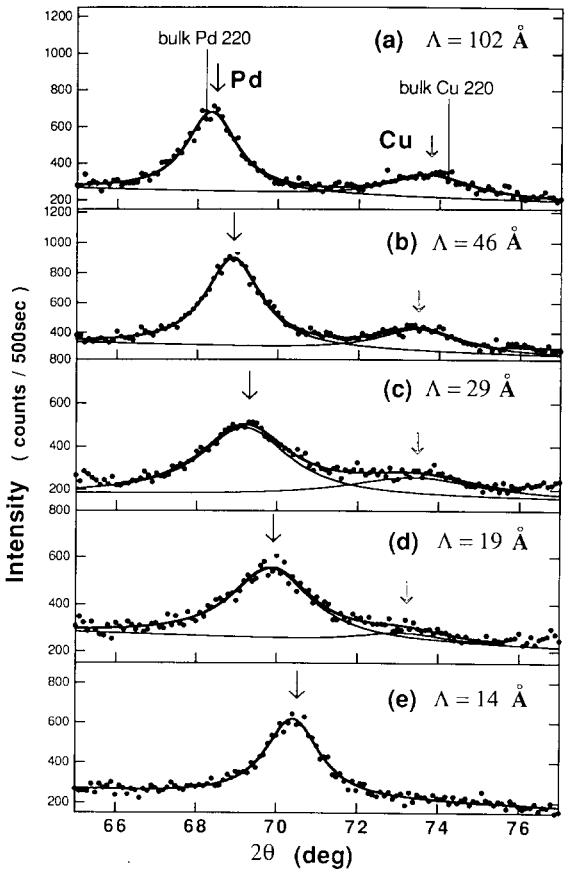

Fig. 4. X-ray diffraction profiles with the scattering vector making an angle of 5° from the film plane for $[Pd(x\text{Å})/Cu(x\text{Å})]_n$ superlattices observed in the grazing incidence geometry. Line plots are the results of profile fitting to estimate peak positions and widths. A modified Lorenztian profile function $[1 + a(x - x_0)^2]^{-1.15}$ was assumed.

single peak. The observed thickness dependences are somewhat different from the results of an electron diffraction study reported by Jankowski for samples prepared by sputtering [12]. In his results, in-plane Au and Ni 220 lattice spacings are nearly equal for $\Lambda < 20$ Å. The difference may be ascribed to the sample preparation method or the buffer layer.

For Pd/Cu superlattices, the observed (220) lattice spacing of a sample with $\Lambda = 14$ Å is located on the extrapolated line of Pd (220) lattice spacings. However, it has deviated from the line for Cu. The lattice spacing of Cu layer has changed abruptly in the range between $\Lambda = 19$ and 14 Å. It is to be noted that both Cu and Pd peaks for samples with $\Lambda = 29$ and 19 Å show significant broadening and that the intensity of the Cu 220 peak has been greatly reduced for a sample with $\Lambda = 19$

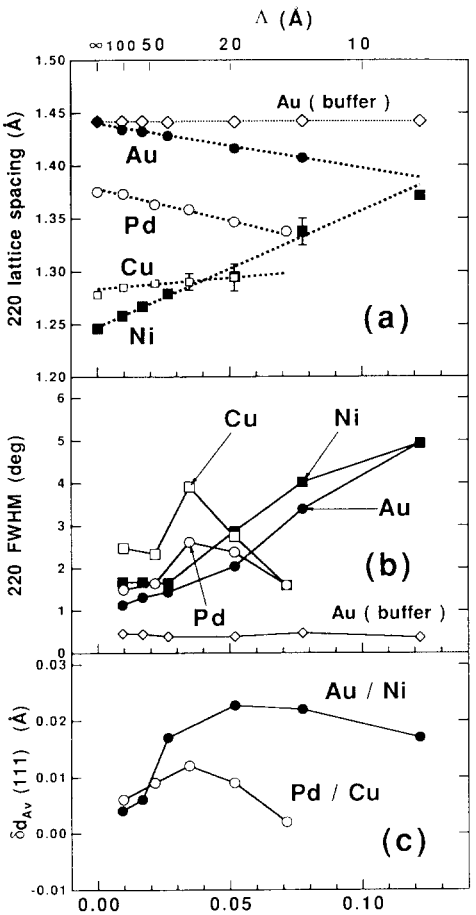

Fig. 5. (a) (220) in-plane lattice spacings, (b) 220 peak widths and (c) deviations of the average (111) lattice spacing from the ideal one plotted as a function of $1/\Lambda$. The dotted lines show the least squares. The solid lines are guides to the eye.

Å. It seems that Cu layers with different lattice spacings coexist particularly in a sample with $\Lambda = 19$ Å.

Finally the observed thickness dependences of in-plane lattice spacings were compared with the observed average (111) lattice spacings (d_{AV}) along the growth direction. Fig. 5(c) shows the deviations of d_{AV} from the ideal lattice spacings expected from the (111) lattice spacings in the bulk metals (d^A, d^B) and the designed individual layer thicknesses (D_A, D_B). The deviation δd_{AV} is given by

$$\delta d_{AV} = d_{AV} - d^A d^B (D_A + D_B)/(D_A d^B + D_B d^A).$$

All the samples showed positive values of δd_{AV}. For Pd/Cu superlattices, the deviation δd_{AV} is the largest at $\Lambda = 29$ Å. The observed abrupt change of the in-plane Cu lattice spacing below $\Lambda = 19$ Å does not directly correlate with the increase of δd_{AV}. However, the structural change in Cu layers seems to be substantial for the increase of δd_{AV}. Particularly, a peak broadening of the in-plane Cu 220 diffraction peak is observed at around $\Lambda = 29$ Å. Also for Au/Ni superlattices, δd_{AV} increases in the range below $\Lambda = 20$ Å where peak broadening is observed.

In summary, we have observed quasi-linear dependences of in-plane lattice spacings on $1/\Lambda$ for Au/Ni and Pd/Cu superlattices with $[111]_{fcc}$ textures. With decrease of Λ, the Au and Pd layers are compressed and Ni and Cu layers are expanded. For Au/Ni superlattices, in-plane lattice spacings of Au and Ni layers become nearly equal at $\Lambda = 8$ Å with the continuous changes of in-plane lattice spacings. The in-plane lattice strains at $\Lambda = 8$ Å are -5% and $+10\%$ for Au and Ni layers, respectively. For Pd/Cu superlattices, the incoherent structure turns to a coherent one at $\Lambda = 14$ Å with an abrupt change of Cu lattice spacing below $\Lambda = 19$ Å. However, the variation of Pd lattice spacings is continuous. The observed in-plane lattice strains at $\Lambda = 14$ Å are -3% and $+5\%$ for Pd and Cu layers, respectively. The analyses of the lattice spacings along the growth direction for individual layers are necessary to clarify the more details of lattice strains in these superlattices. The structure refinements are in progress using a computer program developed by Fullerton et al. [13].

Acknowledgements: This work was supported in part by the grant-in-aid for Scientific Research on Priority Areas (No. 03240103 and 04224103) from Japanese Ministry of Education, Science and Culture. The work at the University Arizona was supported by ONR Grant N0014-91-J-1104. The authours also acknowledge the Japan–US exchange program supported by JSPS and NSF.

References

[1] A.F. Jankowski, J. Phys. F; Metal Physics 18 (1988) 413, Superlattices and Microstructures 6 (1989) 427.
[2] E.M. Gyorgy, D.B. McWhan, J.F. Dillon, Jr., L.R. Walker and J.V. Waszczak, Phys. Rev. B 25 (1982) 6739.
[3] I. Moritani, N. Nakayama and T. Shinjo, J. Phys.: Condensed Matter 2 (1990) 9717.
[4] N. Nakayama, T. Okuyama and T. Shinjo, J. Phys.: Condensed Matter 5 (1993) 1173.
[5] L. Wu, N. Nakayama, B.N. Engel, T. Shinjo and C.M. Falco, Jpn. J. Appl. Phys. (1993, submitted).
[6] D.B. McWhan, M. Gurvitch, J.M. Rowell and L.R. Walker, J. Appl. Phys. 54 (1983) 3886.
[7] J.A. Bain, L.J. Chyung, S. Brennan and B.M. Clemens, Phys. Rev. B 44 (1991) 1184.
[8] M.W.C. Yang, T. Tsakalacos and J.E. Hilliard, J. Appl. Phys. 48 (1977) 876.

[9] H. Konishi, Y. Fujii, N. Hamaya, H. Kawada, Y. Ohishi, N. Nakayama, L. Wu, H. Dohnomae, T. Shinjo and T. Matsushita, Rev. Sci. Instrum. 63 (1992) 1035.
[10] J.R. Dutcher, S. Lee, J. Kim, G.I. Stegeman and C.M. Falco, Mat. Res. Soc. Symp. Proc. 160 (1990) 179.
[11] H. Dohnomae, N. Nakayama and T. Shinjo, Materials Trans. JIM 31 (1990) 615.
[12] A.F. Jankowski, J. Appl. Phys.71 (1992) 1782.
[13] E.E. Fullerton, I.K. Schuller, H. Vanderstraeten and Y. Bruynseraede, Phys. Rev. B 45 (1992) 9292.